Correlation of the Structures and Electronic Spectra of the μ-Peroxo- and μ-Superoxobis[(diethylenetriamine)(ethylenediamine)cobalt(III)] Ions

D. D. DEXTER, C. N. SUTHERBY, M. W. GRIEB [1], and R. C. BEAUMONT*

Department of Chemistry, Alma College, Alma, Mich. 48801, U.S.A.

Received October 7, 1983

The X-ray crystallographic determination of [(en)(dien)CoO_2Co(dien)(en)]$(ClO_4)_2Cl_3 \cdot 2H_2O$ (en = ethylenediamine, dien = diethylenetriamine) allows comparison with previously determined [(en)(dien)(CoO_2Co(dien)(en)]$(ClO_4)_4$. The nearly identical structure of the two bridged cations features reduced intramolecular hydrogen bonding but retains a flat CoO_2Co group whose plane is at 45° relative to the Co–N bond axes cis *to the dioxygen bridge. The π interactions are shown to require development of a model featuring equal participation of two 3d orbitals for each cobalt atom. Hückel calculations are in qualitative agreement with the model, the observed ultraviolet and visible spectra, and with previous EPR determinations for similar compounds.*

Introduction

The relationship of structure and bonding in dioxygen-bridged cobalt amine complexes has long been a subject of interest to many inorganic chemists. Previous structural analyses and UV-visible spectral interpretations have been made on a wide variety of peroxide- and superoxide-bridged complexes and mononuclear dioxygen adducts [2–15]. Direct comparison of the bridged complexes has been seldom possible due sometimes to instability of one of the members of the pair and, on occasion, to a change in structure from a 'bent' CoO_2Co group when O_2 is peroxide to a planar group when O_2 is formally superoxide [2, 6, 7, 16]. The stabilities of the peroxo-bridged [(en)(dien)CoO_2Co(dien)(en)]$^{4+}$ = [I] and of the corresponding +5 charged superoxo-bridged complex [II] hence offer a good opportunity for study of the CoO_2Co group in the two oxidation states. The structure of [I] $(ClO_4)_4$ has already been determined [2].

While the major determiner of stability in such complexes is the electronic structure of the CoO_2Co group, a further consideration is intramolecular hydrogen bonding. When amines fill the coordination positions *cis* to the O_2 bridge, intramolecular hydrogen bonding can occur between these amine hydrogens and the oxygen of the bridge which is bonded to the opposing cobalt (see Fig. 2) [2, 3]. The extent of this hydrogen bonding must be expected to be dependent on the nature of the ligands and on the electronic structure and geometry of the CoO_2Co group.

EPR spectra of a number of superoxide-containing cobalt(III) complexes, both mononuclear and binuclear, have been obtained [10, 17–21]. While

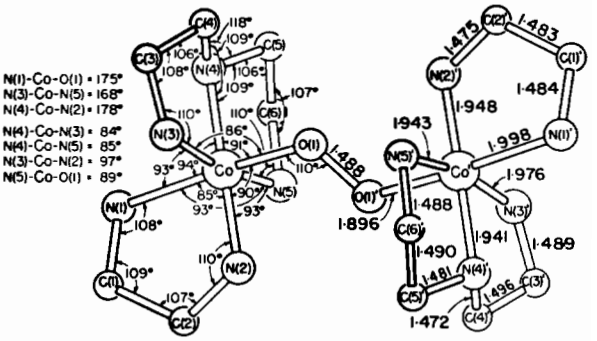

Fig. 1. Bond distances and angles for $[(Co(dien)(en)O]_2^{4+}$. Reprinted with permission from ref. 2. Copyright 1973 American Chemical Society.

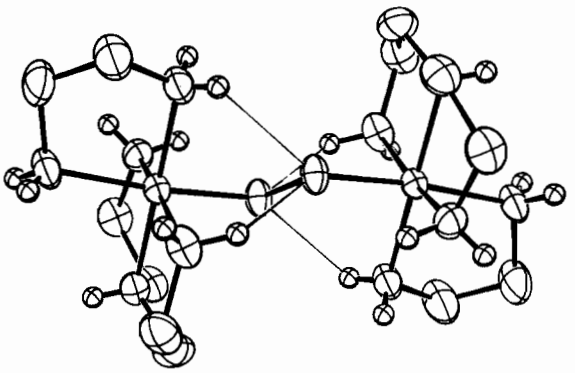

Fig. 2. Structure of $[Co(dien)(en)O]_2^{4+}$ including intramolecular hydrogen bonding [2]. Reprinted in part with permission from ref. 2. Copyright 1973 American Chemical Society.

*Author to whom all correspondence should be addressed.

0020-1693/84/$3.00

spectral analyses have indicated that the unpaired electron resides in a π^* orbital located principally on dioxygen, there have been several theories advanced concerning the principal mode of hyperfine coupling between that electron and the ^{59}Co nucleus. The models proposed have featured π interaction between the π_v^* orbital of O_2^- containing the unpaired electron with one of the cobalt 3d orbitals, *i.e.* the $3d_{xz}$, with interaction occurring between the filled dioxygen π_h^* orbital and the $3d_{z^2}$ orbitals.

Jezowska-Trzebiatowska *et al.* have reported the result of an SCCC MO calculation upon $[(NH_3)_5CoO_2Co(NH_3)_5]^{4+}$ for which their model was a planar CoO_2Co group at 90° with the amine nitrogens [22].

We will suggest an adjusted model for the CoO_2Co system which will be consistent with the observed structures and spectra of the complexes in both oxidation states. The model will be seen to be most like those derived by Wayland and Abd-Elmageed [10] for phosphine and dioxygen adducts of tetraphenylporphinecobalt(II) and by Lever and Gray in a general review of dioxygen complexes [13]. The model will be used for calculation of approximate eigenvalues and eigenvectors for correlation with the observed spectral information.

Experimental

Preparation of Compounds

Descriptions of the preparation of similar peroxide-bridged dicobalt(III) complexes have appeared elsewhere [11, 17, 23–25]. Consistent with these, $[I]Cl_4 \cdot 6H_2O$ may be prepared by slow addition (20 minutes) of a one-tenth mole each mixture of ethylenediamine and diethylenetriamine in 25 ml water to a rapidly aerated (*circa* 200 ml/min through a glass frit) solution containing one-tenth mole of cobalt(II) chloride in 75 ml water. Subsequent chilling overnight yields the first crop of crystals which may be filtered out, washed with ethanol, and air-dried. A second, smaller crop, can be obtained by slow addition (4 hours) of 400 ml ethanol and continued chilling at ice temperature. Total yield, 21 g (58%). *Anal.* Found: 16.21% Co, 19.61% Cl, 4.33% O_2, 19.14% N, 20.01% C, 7.62% H, 14.93% H_2O. Calcd: 16.23% Co, 19.52% Cl, 4.41% O_2, 19.29% N, 19.84% C, 7.49% H, 14.88% H_2O.

Preparations of superoxide compounds [II] are readily achieved by addition of an oxidizing agent to cold aqueous solutions of I under conditions appropriate to each compound [17, 23]. $[II]Cl_5 \cdot 3H_2O$ is prepared by dissolving 1 mmol of $[I]Cl_4 \cdot 6H_2O$ (0.72 g) in 120 ml 50% v/v ethanol/water cooled to ice temperature. After addition of two drops of 12 *M* HCl, chlorine gas is bubbled slowly through the solution (about 30 ml/min) for ten minutes, during which time the solution changes from deep brown to deep green. Concentrated HCl (50 ml) and then ethanol (170 ml) are added, after which the mixture is left in an ice bath for an hour. The green crystals are filtered with a sintered glass crucible, washed with ethanol, and air-dried, giving a yield of 0.65 g of $[II]Cl_5 \cdot 3H_2O$ (92%). Observed results of element analysis: 16.36% Co, 25.35% Cl, 4.59% O_2, 18.68% N, 20.23% C, 6.65% H. Calculated percentages: 16.66% Co, 25.05% Cl, 4.52% O_2, 19.80% N, 20.36% C, 6.84% H.

$[II](ClO_4)_5 \cdot 5H_2O$ may be prepared by dissolving 0.71 g of $[II]Cl_5 \cdot 3H_2O$, 1.0 mmol in 50 ml water acidified with one drop 70% $HClO_4$. After filtration, the solution is placed in an ice bath and 7 ml 70% $HClO_4$ is added with stirring. The light green crystals are filtered, washed with chloroform, and then dried in partial vacuum over calcium chloride. Yield: 0.83 g (98%). The compound slowly decomposes and light accelerates this change to an orange, unidentified substance. Observed results of element analysis: 3.04% O_2, 13.04% N, 14.61% C, 4.96% H. Calculated percentages: 3.01% O_2, 13.16% N, 13.56% C, 4.92% H.

Crystals of $[II](ClO_4)_2 \cdot Cl_3 \cdot 2H_2O$ suitable for X-ray analysis can be prepared from $[II](ClO_4)_5 \cdot 5H_2O$ by allowing a solution of 0.050 g of the latter in 10 ml 1:1 v/v water/ethanol acidified with 3 drops 12 *M* HCl to evaporate slowly. The element composition was revealed by the X-ray-determined structure of the compound.

Element Analysis and Formulas

Cobalt was analyzed by slowly heating weighed samples of the compounds in crucibles to 750–800 °C followed by immediate weighing as Co_2O_3 or as Co_3O_4 following continued heating for one week [26]. Cobalt analyses were not performed on the perchlorate salts due to their explosive tendency when heated.

Chloride was determined gravimetrically as AgCl. Carbon, hydrogen, and nitrogen analyses were performed by the Alfred Bernhardt Microanalytical Laboratory of Elbach, West Germany. Water analysis was made by observation of weight loss at 100 °C to avoid decomposition of the dioxygen bridge at higher temperatures.

Dioxygen was determined gasometrically by measurement of the volume of gas released upon addition of 10 ml saturated $K_3[Fe(CN)_6]$ to 0.5 mmol solid samples within a closed system initially in a thermostated water bath. The system was removed from the bath, the reaction vessel was heated to boiling, following which the system was returned to the bath.

Formulas for the compounds were estimated using the minimum molecular weight method of Harwood [27] upon the several results of analysis for each compound. Waters of crystallization were rounded off to the nearest whole number.

UV-Visible Spectra

Spectra in the 200 to 750 nm region were recorded with a GCA/McPherson 721 spectrophotometer using 10^{-2} to 10^{-5} *M* solutions of I and II chlorides in 1 cm silica cells. For wavelengths beyond 750 nm, 1 cm glass cells were used in a Beckman DU spectrophotometer. The solution of the corresponding mononuclear hydroxo complex $[Co(dien)(en)OH]^{2+}$ was prepared by addition of a slight excess of 0.1 *M* NaOH to $[Co(dien)(en)Cl]Cl_2$ prepared previously [23, 28, 29]. Solutions of $[Co(en)_3]^{3+}$ were prepared by dissolving $[Co(en)_3]Cl_3$ in water [30].

X-Ray Data Collection

Crystal data for $[II](ClO_4)_2 \cdot Cl_3 \cdot 2H_2O$ are given in Table I. A prismatic specimen of approximate dimensions 0.2 × 0.2 × 0.3 mm was mounted in arbitrary orientation on a Syntex $P2_1$ diffractometer. With the crystal bathed in a stream of liquid nitrogen vapor, the intensities of the 2440 unique reflections accessible to monochromatized Cu-Kα radiation ($2\theta_{max}$ = 138.3°) were measured with step scans [31]. The 1713 reflections having $I_o > 2\,(I_o)$ (based on counting statistics) were considered observed. The intensities were corrected for absorption.

Structure Determination

The structure was determined from difference maps after the single Co atom in the asymmetric unit was located from an $E^2 - 1$ vector map. After anisotropic temperature factors for all non-hydrogen atoms had been introduced, hydrogen atoms were located in a difference map and were included in the least-squares refinement with isotropic temperature factors fixed at 2.0 Å^2 [31]. Corrections for the anomalous dispersion of Co [32] were included and statistical weights were used. The function minimized, $\Sigma w(|F_o| - |F_c|)^2$, converged with $\Sigma[||F_o| - |F_c||]/\Sigma|F_o| = 0.085$ and $[\Sigma w(|F_o| - |F_c|)^2/wF_o^2]^{1/2} = 0.090$ for the observed reflections. The final difference map was flat except for a residual peak at the Co position. Local implementation on a PDP-11/70 of ORTEP [33] and of Shiono's [34] programs were used for most of the calculations.

Molecular Orbital Calculations

The simple Hückel method was employed separately upon the CoO_2Co σ and π systems using a version of EIGQR [35] modified for use on a PDP-11/70 computer. Values employed for the coulomb integrals α_{Co} were −11.2 and −13.86 eV, respectively for e_g and t_{2g} orbitals, respectively, while −13.6 was used for α_O. The oxygen–oxygen resonance integral was assigned −1.6 eV for both the σ and π systems in the superoxo complex and −1.2 eV in the peroxo complex.

For the π system, the value of the cobalt–oxygen resonance integral, $\beta_{CoO}(\pi)$, was set at −0.7 eV for each of the O2p–Co3d interactions. The secular determinant was 6 × 6 with two (orthogonal) cobalt orbitals interacting with one oxygen orbital [36]. For the σ system, $\beta_{CoO}(\sigma)$ was set at −2.0 eV.

Results and Discussion

Structures

Crystal data obtained in this study are in Table I, coordinates and thermal parameters are presented in Table II, bond distances and angles in Table III, and torsion angles about non-hydrogen bonds in Table IV. The numbering scheme and geometry of the Co–O–O–Co group appear in Fig. 3 and a packing diagram in Fig. 4. Intra- and intermolecular hydrogen bonding and close contacts are included in Table V and are indicated as thin lines in Fig. 4.

TABLE I. Crystal Data for $[(en)(dien)CoO_2Co(dien)(en)](ClO_4)_2Cl_3 \cdot 2H_2O$.

Formula weight	817.79
Space group	$P2_1/C$
U	1562.31 Å^3
D_c	1.738 g·cm^{-3}
Z	2
μ	126.7 cm^{-1}
a	8.811(1) Å
b	11.535(1) Å
c	16.477(1) Å
β	68.894(6) deg

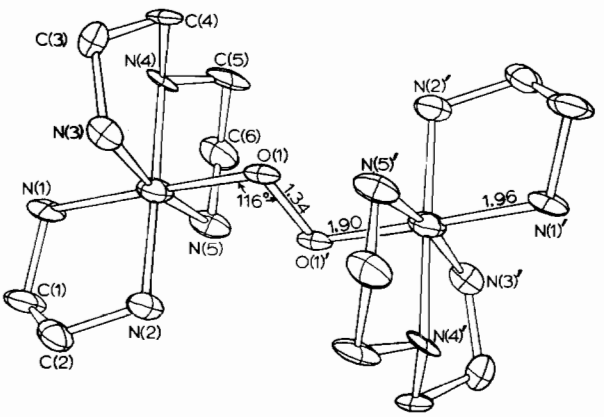

Fig. 3. ORTEP drawing of $[Co(dien)(en)O]_2^{5+}$ showing skeletal arrangement and CoO_2Co distances and angles.

That the bridging dioxygen in II is best considered a superoxide is readily deduced by comparison of the observed 1.34 Å bond distance with the 1.49 Å distance in the peroxide complex I. This is in agreement with the decaammine peroxide- and superoxide-bridged complexes [3, 7].

TABLE II. Positional and Thermal Parameters and their Estimated Standard Deviations.[a]

Atom	*X*	*Y*	*Z*	*B*(1,1)	*B*(2,2)	*B*(3,3)	*B*(1,2)	*B*(1,3)	*B*(2,3)
Co	0.4447(3)	0.1916(3)	−0.0064(2)	0.0008(5)	0.0037(2)	0.0021(1)	−0.0001(3)	−0.0004(2)	0.0002(1)
Cl(1)	0.1882(6)	0.0965(4)	0.3046(3)	0.0013(8)	0.0053(4)	0.0022(2)	−0.0002(4)	−0.0004(3)	0.0000(2)
Cl(2)	0.6218(6)	−0.0042(4)	0.3509(3)	0.0027(8)	0.0040(4)	0.0027(2)	−0.0004(4)	−0.0014(3)	0.0002(2)
Cl(3)	0.0	0.0	0.0	0.002(1)	0.0058(6)	0.0028(3)	0.0004(6)	−0.0009(4)	−0.0006(3)
O(1)	0.547(1)	0.046(1)	−0.0008(8)	0.003(2)	0.0042(1)	0.0030(6)	−0.001(1)	0.0003(9)	−0.0002(6)
O(2)	0.175(2)	0.213(1)	0.337(1)	0.004(2)	0.005(1)	0.0049(8)	−0.000(1)	−0.001(1)	−0.0019(8)
O(3)	0.053(2)	0.069(1)	0.2798(9)	0.004(3)	0.011(2)	0.0038(7)	−0.002(2)	−0.003(1)	−0.0006(9)
O(4)	0.337(2)	0.086(1)	0.2282(8)	0.003(2)	0.009(1)	0.0026(6)	0.001(1)	0.0005(8)	−0.0003(7)
O(5)	0.803(2)	0.518(1)	0.129(1)	0.012(3)	0.009(2)	0.0034(7)	0.000(2)	−0.001(1)	−0.0023(8)
O(6)	0.710(2)	0.095(1)	0.1604(8)	0.005(2)	0.008(1)	0.0025(6)	0.002(1)	0.0003(9)	0.0006(7)
N(1)	0.335(2)	0.341(1)	−0.004(1)	0.003(3)	0.005(1)	0.0027(7)	−0.000(1)	−0.001(1)	0.0005(8)
N(2)	0.236(2)	0.141(1)	0.079(1)	0.005(3)	0.006(1)	0.0027(7)	−0.001(2)	−0.001(1)	−0.0004(8)
N(3)	0.532(2)	0.244(1)	0.0817(9)	0.002(3)	0.004(1)	0.0024(6)	0.000(1)	−0.000(1)	−0.0002(7)
N(4)	0.648(2)	0.247(1)	−0.090(1)	0.001(3)	0.005(1)	0.0025(7)	0.001(1)	−0.001(1)	−0.0008(8)
N(5)	0.399(2)	0.139(1)	−0.109(1)	0.003(3)	0.006(1)	0.0031(7)	−0.001(1)	−0.002(1)	0.0007(8)
C(1)	0.155(2)	0.327(2)	0.041(1)	0.001(3)	0.005(2)	0.0031(9)	0.000(2)	−0.000(1)	0.000(1)
C(2)	0.130(2)	0.244(2)	0.115(1)	0.005(3)	0.006(2)	0.0030(8)	−0.000(2)	−0.000(1)	−0.000(1)
C(3)	0.693(2)	0.304(2)	0.039(1)	0.004(3)	0.004(2)	0.004(1)	−0.000(2)	−0.002(1)	−0.001(1)
C(4)	0.773(2)	0.244(2)	−0.047(1)	0.002(3)	0.005(2)	0.004(1)	−0.002(2)	−0.002(1)	0.001(1)
C(5)	0.687(2)	0.181(2)	−0.173(1)	0.003(4)	0.008(2)	0.004(1)	0.000(2)	−0.002(1)	0.000(1)
C(6)	0.532(2)	0.177(2)	−0.191(1)	0.005(3)	0.006(2)	0.0019(8)	0.002(2)	−0.002(1)	−0.000(1)
H(1)	0.37(2)	0.38(2)	−0.06(1)						
H(2)	0.40(2)	0.38(2)	0.03(1)						
H(3)	0.26(2)	0.11(2)	0.12(1)						
H(4)	0.18(2)	0.09(2)	0.05(1)						
H(5)	0.53(2)	0.17(2)	0.11(1)						
H(6)	0.47(2)	0.31(2)	0.12(1)						
H(7)	0.63(2)	0.34(2)	−0.10(1)						
H(8)	0.32(2)	0.14(2)	−0.12(1)						
H(9)	0.39(2)	0.06(2)	−0.10(1)						
H(10)	0.12(2)	0.31(2)	−0.01(1)						
H(11)	0.10(2)	0.41(2)	0.07(1)						
H(12)	0.16(2)	0.28(2)	0.16(1)						
H(13)	0.01(2)	0.22(2)	0.15(1)						
H(14)	0.77(2)	0.30(2)	0.08(1)						
H(15)	0.68(2)	0.40(2)	0.03(1)						
H(16)	0.86(2)	0.30(2)	−0.08(1)						

H(17)	0.81(2)	0.16(2)	−0.05(1)
H(18)	0.71(2)	0.11(2)	−0.16(1)
H(19)	0.77(2)	0.22(2)	−0.22(1)
H(20)	0.50(2)	0.26(2)	−0.20(1)
H(21)	0.54(2)	0.11(2)	−0.23(1)
H(22)	0.71(2)	0.07(2)	0.22(1)
H(23)	0.79(2)	0.07(2)	0.13(1)
H(21)	0.54(2)	0.11(2)	−0.23(1)
H(22)	0.71(2)	0.07(2)	0.22(1)
H(23)	0.79(2)	0.07(2)	0.13(1)

[a] The form of the anisotropic thermal parameter is $\exp[-B(1,1)h^2 + B(2,2)k^2 + B(3,3)l^2 + 2B(1,2)hk + 2B(1,3)hl + 2B(2,3)kl)]$.

TABLE III. Bond Distances and Angles involving non-Hydrogen Atoms.

Distances (Å)	
Co–O(1)	1.897(12)
Co–N(1)	1.958(17)
Co–N(2)	1.962(15)
Co–N(3)	1.959(15)
Co–N(4)	1.935(16)
Co–N(5)	1.977(18)
O(1)–O(1)	1.336(17)
N(1)–C(1)	1.490(28)
N(2)–C(2)	1.495(24)
N(3)–C(3)	1.519(24)
N(4)–C(4)	1.510(25)
N(4)–C(5)	1.485(25)
N(5)–C(6)	1.521(26)
C(1)–C(2)	1.501(29)
C(3)–C(4)	1.518(28)
C(5)–C(6)	1.482(28)
Cl(1)–O(2)	1.446(15)
Cl(1)–O(3)	1.447(17)
Cl(1)–O(4)	1.476(15)
Cl(1)–O(5)	1.452(16)
Angles (°)	
O(1)–O(1)–Co	116.1(9)
O(1)–Co–N(1)	176.1(6)
O(1)–Co–N(2)	91.8(6)
O(1)–Co–N(3)	85.8(6)
O(1)–Co–N(4)	90.3(6)
O(1)–Co–N(5)	90.7(6)
N(1)–Co–N(2)	85.3(7)
N(1)–Co–N(3)	91.9(7)
N(1)–Co–N(4)	92.7(7)
N(1)–Co–N(5)	92.0(7)
N(2)–Co–N(3)	93.8(6)
N(2)–Co–N(4)	177.9(7)
N(2)–Co–N(5)	95.1(7)
N(3)–Co–N(4)	85.8(6)
N(3)–Co–N(5)	170.5(7)
N(4)–Co–N(5)	85.3(7)
Co–N(1)–C(1)	110(1)
Co–N(2)–C(2)	109(1)
Co–N(3)–C(3)	111(1)
Co–N(4)–C(4)	107(1)
Co–N(4)–C(5)	110(1)
Co–N(5)–C(6)	109(1)
N(1)–C(1)–C(2)	106(2)
C(1)–C(2)–N(2)	107(2)
N(3)–C(3)–C(4)	105(2)
C(3)–C(4)–N(4)	105(2)
N(4)–C(5)–C(6)	105(2)
O(2)–Cl(1)–O(3)	109.5(9)
O(2)–Cl(1)–O(4)	110.0(8)
O(2)–Cl(1)–O(5)	108.7(9)
O(3)–Cl(1)–O(4)	108.8(9)
O(3)–Cl(1)–O(5)	110.6(9)
O(4)–Cl(1)–O(5)	109.2(9)

TABLE IV. Torsion Angles.

	(superoxo complex) This work	(peroxo complex) Fritch, Christoph & Shaefer
O(1)'–O(1)–Co–N(1)	83	69
O(1)'–O(1)–Co–N(2)	42	45
O(1)'–O(1)–Co–N(3)	136	142
O(1)'–O(1)–Co–N(4)	–138	–133
O(1)'–O(1)–Co–N(5)	–53	–48
O(1)–Co–N(1)–C(1)	–54	–13
O(1)–Co–N(2)–C(2)	163	–165
O(1)–Co–N(3)–C(3)	95	95
O(1)–Co–N(4)–C(4)	–60	–61
O(1)–Co–N(4)–C(5)	67	69
O(1)–Co–N(5)–C(6)	–94	–99
Co–N(1)–C(1)–C(2)	37	–36
Co–N(2)–C(2)–C(1)	39	–41
Co–N(3)–C(3)–C(4)	–33	–31
Co–N(4)–C(4)–C(5)	–49	–48
Co–N(4)–C(5)–C(6)	46	44
Co–N(5)–C(6)–C(5)	31	35
N(1)–C(1)–C(2)–N(2)	–49	50
N(3)–C(3)–C(4)–N(4)	53	50
N(4)–C(5)–C(6)–N(5)	–49	–51
C(3)–C(4)–N(4)–C(5)	–172	–172
C(4)–N(4)–C(5)–C(6)	168	169

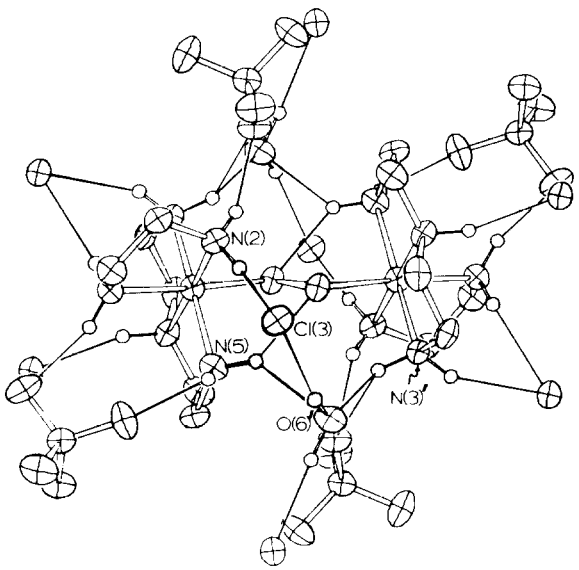

Fig. 4. Drawing of $[Co(dien)(en)O]_2(ClO_4)_2Cl_3 \cdot 2H_2O$ indicating crystal packing and hydrogen interactions.

A small but possibly significant distance change is associated with Co(1)–O(1) and Co(1)–N(1). In going from peroxide to superoxide, the Co(1)–O(1) distance remains constant at 1.90 Å while the Co(1)–N(1) distance decreases from 1.998 to 1.958(17) Å. While the constancy of the Co(1)–O(1) bond length can be explained as due to a mutual cancellation of the increase in electrostatic repulsion with a shortening effect due to π bond formation when O_2^{2-} changes to O_2^-, the decrease in Co(1)–N(1) distance suggests a weak (sigma) *trans*-effect which has been observed when other ligands are present [2, 3]. The remaining Co–N distances average 1.952 Å in the peroxide I and 1.954 Å in the superoxide II. Thus while the increase in oxidation state has essentially no effect on these other four cobalt–nitrogen bonding interactions, it reduces the sigma donor nature of dioxygen from being stronger than to being approximately equivalent with that of a primary amine.

Bond angles about the cobalt centers I and II reveal quite similar moderate distortion from pure octahedral symmetry. The N(1)–Co(1)–N(2) angle associated with the ethylenediamine is 85° in both I and II. Similarly, the N(3)–Co(1)–N(4) and N(4)–Co(1)–N(5) angles are essentially invariant between the two oxidation states. These distortions from 90° can probably be attributed to the 'bite' sizes of the ligands rather than to electronic configuration.

The increase of the Co(1)–O(1)–O(1)' angle from 110° in I to 116° in II can be rationalized in two non-exclusive ways. One is that removal of an electron from O_2^{2-} to form O_2^- causes reorganization to a configuration using oxygen sp^2 hybrid orbitals within the CoO_2Co plane. Such rearrangement does not seem likely in view of the unchanged Co(1)–O(1) bond length, for an sp^2 hybrid orbital would presumably have greater sigma overlap than a π or π^* orbital. A simpler and perhaps sufficient explanation is that the bridging O_2^- is less able than O_2^{2-} to shield the two positive cobalt(III) centers from one another; this increase in repulsion results in an increased torque upon the O_2 bridge. With the loss of an electron, dioxygen becomes less effective as a sigma donor.

As in the peroxide, the CoO_2Co group in II is planar. This, coupled with the same N(2)–Co(1)–O(1)–O(1)' dihedral angle (45° in both complexes) suggests that the spatial arrangement of the basis atomic orbitals of the CoO_2Co system must be the same. The 45° angle brings the π_v^* orbitals of the O_2 bridge into equal interaction with *two* 3d orbitals on each cobalt atom. The consequences of this will be considered in the discussion of the electronic spectra, Hückel calculations, and EPR spectra.

Hydrogen bonding appears to play a role in the stabilities of both the peroxide and superoxide complexes. Fritch, Christoph, and Schaefer observed intramolecular hydrogen sharing in I between one hydrogen each from N(2) and N(5) and O(1)' and between N(2)' and N(5)' and O(1) [2]. Similar intramolecular hydrogen bonding was observed by Schaefer and Marsh in $[(NH_3)_5CoO_2Co(NH_3)_5]^{5+}$ [3].

We find in II that intramolecular hydrogen bonding is less significant in that only two H-bonds occur: between one hydrogen of N(5) and O(1)′ and between N(5)′ and O(1). Additional stability of solid II in the crystalline solid seems to be derived from the interactions among the perchlorate, chloride and water molecules involved with amine hydrogens in a network of hydrogen bonds which also hold the crystal together. Most notably, the water oxygen, O(6), accepts H-bonds from N(3) and N(5)′ while donating hydrogen bonds to Cl(2) and Cl(3) which in turn bridges to H(4) on N(2). That this stabilization persists in aqueous solution is suggested by the observation of Ferrer, Hand, and Sykes that the rates of decomposition of both $[(NH_3)_5CoO_2Co(NH_3)_5]^{4+,5+}$ are inversely dependent on hydrogen and anion concentrations [37].

With the exception of the ethylenediamine ring, the torsion angles listed in Table IV confirm the expected similarity between the conformations of I and II. In II this ring has adopted the opposite enantiomeric form, probably in response to the H-bonding requirements of this particular salt.

A Model for the CoO_2Co System

Because of the observed structures for I and II, a model for orbital involvement in the CoO_2Co systems can be developed. First, the dioxygen portions of the complexes can be formulated as peroxide and superoxide ions containing four and three electrons, respectively in the π and π^* orbitals which would each be doubly degenerate in a symmetric environment. The sigma orbitals internal to dioxygen are conventionally assumed to contain little 2s character; thus only σ^* (2p–2p) is vacant but at a potential energy significantly greater than that of the π^* orbitals [36b]. The lowering of symmetry in formation of the CoO_2Co fragment removes the degeneracy of the π-type orbitals; it is convenient to relabel these dioxygen orbitals as π_h, π_h^*, π_v, and π_v^* [9, 11, 13].

The two cobalt(III)–amine fragments can also be treated in a conventional manner. If the $3d_{z^2}$ orbital of each is held vacant as the potential receptor site for sigma donation from dioxygen, then six electrons must be placed in the orbitals $3d_{xz}$, $3d_{yz}$, and $3d_{xy}$.

In bringing together the fragments to form the planar CoO_2Co portion of the complexes with the observed in-plane and dihedral angles, one readily observes that maximal cobalt–oxygen sigma overlap is achieved using the π_h and π_h^* dioxygen orbitals in the CoO_2Co plane. An accurate accounting for the sigma interactions would include contributions from $3d_{xz}$ and $3d_{yz}$ and 4s in combination with $3d_{z^2}$. For simplicity, we considered the sigma system to employ only d_{z^2} from cobalt. Thus the sigma system is approximately based upon the atomic orbitals $3d_{z^2}$(Co)–2p(O)–2p(O)–$3d_{z^2}$(Co) while the actual character of the overlap between atoms is σ–π–σ.

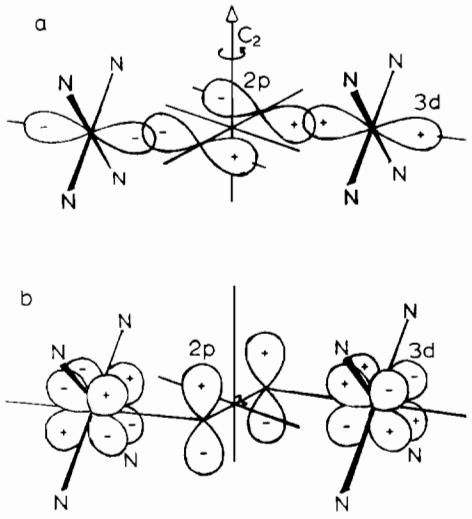

Fig. 5. (a) Sigma interaction of dioxygen orbital with cobalt $3d_{z^2}$ resulting in the σ_u orbital (σ_g, σ_u^*, and σ_g^* not shown). (b) Pi interaction of dioxygen orbitals with cobalt $3d_{xz}$ and $3d_{yz}$ resulting in the π_u orbital (π_g, π_3, π_4, π_u^*, π_g^* not shown).

Figure 5(a) indicates the orbital interactions which result in four new orbitals labelled for convenience σ_u, σ_g, σ_u^*, and σ_g^*, although none are of truly sigma symmetry. In both the peroxide and superoxide complexes, the four electrons originally in π_h and π_h^* on dioxygen occupy the two orbitals of lower energy.

Overlap of π character is achieved between the π_v and π_v^* orbitals of dioxygen with *both* the $3d_{xz}$ and $3d_{yz}$ of each cobalt. The 45° dihedral angle of N(2)–Co(1)–O(1)–O(1)′ dictates that the cobalt orbitals must be equally $3d_{xz}$ and $3d_{yz}$. The two 3d orbitals together account for the interaction between each oxygen and its neighboring cobalt atom. The basis atomic orbitals are thus $3d_{xz}$, $3d_{yz}$(Co)–$2p_v$(O)–$2p_v$(O)–$3d_{xz}$, $3d_{yz}$(Co). Figure 5(b) illustrates the symmetries of the six basis orbitals which result in molecular orbitals π_u, π_g, π_3, π_4, π_u^*, and π_g^*. In the superoxide-bridged complexes, only one electron is in π_g^*.

This model for the sigma and pi interactions may be applicable to other bridged complexes. Both the planar RuSSRu and TiOOTi groups have been observed to display the 45° angle with *cis* ligands which is indicative of this possibility [38, 39]. Furthermore, mononuclear heme-like dioxygen adducts also display this characteristic angle, with the terminal oxygen having fourfold positional disorder [40]. While steric repulsion between the bridging ligand and those ligands *cis* to it must be significant as the cause of this angle, it is the resulting orbital interactions which are accounted for in our model which shows that both sigma and pi bonding can occur with a 45° dihedral angle as well as at the conventional 90° angle.

TABLE V. Potential H-bond Contacts.

Atoms	A··B	H··B	A–H	Angle AHB
N(3)–H(5)–O(6)	2.92 Å	2.22 Å	0.97 Å	128 deg
N(5)–H(9)–O(1)	2.96	2.25	0.95	130
N(2)–H(3)–O(4)	2.97	2.15	0.98	159
N(5)–H(8)–O(2)	2.97	2.27	0.95	129
N(3)–H(5)–O(4)	3.02	2.28	0.97	132
N(5)–H(9)–O(6)	3.08	2.37	0.95	131
O(6)–H(23)–Cl(3)	3.14	2.37	1.06	167
N(4)–H(7)–Cl(2)	3.15	2.18	1.00	164
O(6)–H(22)–Cl(2)	3.16	2.22	1.00	156
N(1)–H(1)–O(5)	3.18	2.49	1.04	130
N(3)–H(6)–Cl(2)	3.23	2.31	0.99	153
N(1)–H(2)–Cl(2)	3.23	2.41	1.13	147
N(2)–H(4)–Cl(3)	3.26	2.26	1.02	166

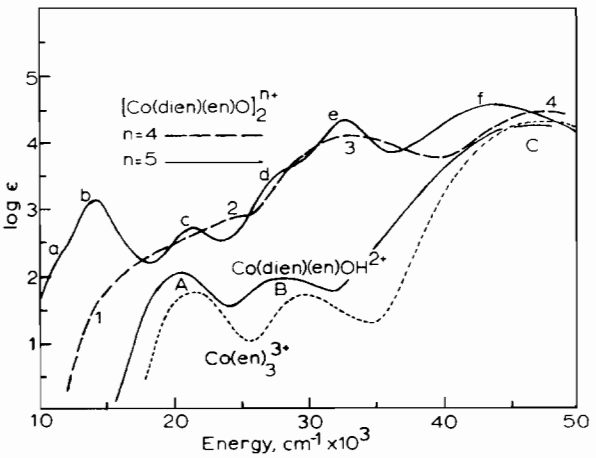

Fig. 6. Visible and ultraviolet spectra of the mononuclear and binuclear complexes.

UV-Visible Spectra

Figure 6 contains the electronic excitation spectra of I and II as well as of the mononuclear species $[Co(dien)(en)OH]^{2+}$ and $[Co(en)_3]^{3+}$. The spectra all are consistent with those observed for analogous complexes [9–11, 14].

A. $[Co(dien)(en)OH]^{2+}$ and $[Co(en)_3]^{3+}$

Peaks A and B of these mononuclear complexes have been assigned to ligand field transitions labelled $^1A_{1g} \rightarrow {}^1T_{1g}$ and $^1A_{1g} \rightarrow {}^1T_{2g}$, respectively, in octahedral symmetry, while the high energy band C near 45,000 cm^{-1} has been assigned to ligand-to-metal $\sigma \rightarrow \sigma^*$ charge transfer [41].

B. $[(en)(dien)CoO_2Co(dien)(en)]^{4+}$

The spectrum of the peroxo complex in Fig. 6 should contain essentially the same ligand field and charge transfer bands as the mononuclear complexes and, additionally, bands associated with electron excitation into the vacant σ_u^* and σ_g^* of the CoO_2Co system described above. Since one would expect only moderate changes in energy and intensity for bands A–C (*i.e.* an increase of about 0.3 in molar absorptivity), it is necessary to recognize four distinguishably new or augmented bands, noted 1–4. Identification of these four bands does not exclude the presence of additional indistinguishable bands.

Band 1 is likely $\pi_g^* \rightarrow \sigma_u^*$. It should be the lowest energy band of more than negligible intensity as is shown in the energy level diagram for the model and in the Hückel calculations (*vide infra*).

Band 2 at 24,000 cm^{-1} has molar absorptivity between 10^2 and 10^3, indicating significantly less forbiddeness to the transition than the ligand field bands of the mononuclear complexes in the same energy region. The energies of σ_g, π_g, π_3, π_4, $3d_{xy} \rightarrow 3d_{x^2-y^2}$ all should come close in energy to that of band 3 as well as should that of $\pi_u^* \rightarrow \sigma_u^*$. However, the degeneracy of π_3 and π_4 and of $3d_{x^2-y^2}$ make it the best candidate for the prominent absorption. Also, inspection of calculated eigenvectors for π_3 and π_4 suggests that they are non-symmetric.

Band 3 has the intensity and broadness commonly associated with charge-transfer but at an energy significantly less than that observed in mononuclear species. Assignment to the $\sigma_g \rightarrow \sigma_u^*$ transition of the CoO_2Co system fits this description and Hückel calculations support the charge transfer character (*vide infra*).

Band 4 may be assigned readily to $\sigma_u \rightarrow \sigma_g^*$ of the CoO_2Co system superimposed upon band *c* of the mononuclear species. The lack of significant shift in going from mononuclear complexes to the peroxo complex is in qualitative agreement with the structural observation that the Co(1)–O(1) distance in the peroxide-bridged complexes is only slightly less than the Co–N and Co–O distances in mononuclear complexes and that the peroxide does induce a slight lengthening of the *trans* Co–N bond.

TABLE VI. Visible and Ultraviolet Absorption Band Assignments.

Energy, $cm^{-1} \times 10^3$	$[Co(dien)(en)OH]^{2+}$			$[Co(dien)(en)O]_2^{4+}$ (I)			$[Co(dien)(en)O]_2^{5+}$ (II)		
	Band	Assignment	Energy	Band	Assignment	Energy	Band	Assignment	Energy
10							a	$\pi_g^* \rightarrow \sigma_u^*$	10.6
				1	$\pi_g^* \rightarrow \sigma_u^*$	14	b	$\pi_u^* \rightarrow \pi_g^*$ and $\pi_u^* \rightarrow 3d_{x^2-y^2}$	14.0
20	A	$'^1A_{1g} \rightarrow {}^1T_{1g}'$	20.5				c	$\pi_3, \pi_4 \rightarrow \pi_g^*, 3d_{x^2-y^2}$	21.3
				2	$\sigma_g, \pi_g, \pi_3, \pi_4 \rightarrow 3d_{x^2-y^2}$ and $\pi_u^* \rightarrow \sigma_u^*$	24	d	$\pi_u^* \rightarrow \sigma_g^*$ and $3d_{xy}, \pi_3, \pi_4 \rightarrow \sigma_u^*$	27
	B	$'^1A_{1g} \rightarrow {}^1T_{2g}'$	27.5						
30				3	$\sigma_g \rightarrow \sigma_u^*$ (of CoO_2Co) and $\pi_g \rightarrow \sigma_u^*$	33	e	$\pi_u \rightarrow \pi_g^*$ and $\pi_g \rightarrow \sigma_u^*$ (superimposed on band 3 in I)	32.6
40							f	$\sigma_u \rightarrow \sigma_g^*$ (of CoO_2Co)	44
	C	$\sigma_g \rightarrow \sigma_u^*$ (N to Co CT)	46.5	4	$\sigma_u \rightarrow \sigma_g^*$ (superimposed on N to Co CT)	47			
50									

C. [(en)(dien)CoO_2(dien)(en)]$^{5+}$

For the most part, the spectrum of the superoxide complex has the appearance of that of the peroxide complex with new bands superimposed; some shifting of bands also seems to have occurred. New or shifted bands are labelled from *a* through *f*. Those bands which are new should be attributable to transitions involving π_g^* as the receptor orbital. Band *b* is most readily explained as $\pi_u^* \rightarrow \pi_g^*$ in agreement with previous assignment for the decaammine complexes by Miskowski *et al.* [9].

In the superoxo complex both the σ_g^* and σ_u^* orbitals should be at a lower energy than in the peroxo complex if charge of the ligand be considered as a main determiner of difference in sigma bond strength. At the same time, shortening of the dioxygen bond distance should raise both π_g^* and π_u^* above their levels in the peroxo complex. Thus band *a* at about 10,600 cm^{-1} represents a shift to lower energy of band *1* of the peroxo complex ($\pi_g^* \rightarrow \sigma_g^*$). Band *c* similarly is assignable to $3d_{xy} \rightarrow \sigma_u^*$ although π_g, π_3, and π_4 occur at nearly the same energy as $3d_{xy}$.

At 27,000 cm^{-1}, band *d* is a pronounced shoulder on the higher energy band *e*; it occurs at approximately the same energy as the $^1A_{1g} \rightarrow {}^1T_{2g}$ transition in mononuclear complexes; however, in the peroxo complex the band is not distinguishable. Both $\pi_u^* \rightarrow \sigma_g^*$ and π_g, π_3, π_4, $3d_{xy} \rightarrow \sigma_u^*$ would occur at near this energy. Of these, transitions involving either or both π_g and π_u^* would move to lower energy in going from the peroxide to the superoxide complex. Assuming that band *d* also occurs in the peroxo complex but is hidden under band *3*, it would become distinguishable by moving to a lower energy. Of the possible assignments, π_3, π_4, $3d_{xy} \rightarrow \sigma_u^*$ would give the narrowest band of greatest intensity.

Band *e* corresponds in energy with band *3* of the peroxo complex but has half again as large an absorption coefficient and a noticeably smaller peak width. The $\sigma_g \rightarrow \sigma_u^*$ transition observed in the peroxo complex should occur here with essentially the same energy, absorption coefficient, and bandwidth. If the $\pi_u \rightarrow \pi_g^*$ band were superimposed, the increased intensity ($\epsilon_e - \epsilon_3 \approx 7 \times 10^3$ where ϵ = molar absorptivity) and relatively narrow bandwidth (*cf.* band *b*) would be explained. That this is the proper assignment is further suggested by the constraint on the maximum energy for π_g^* imposed by the observed potential energy for σ_u^* (*vide infra*). In O_2^- and $HO_2^\cdot$ this band has been variously observed in the region 40–48,000 cm^{-1}. The shift to near 33,000 cm^{-1} in the superoxide-bridged dicobalt complexes can be rationalized as due to lengthening of the dioxygen bond from 1.25–1.3 Å in simple ionic and monocoordinated superoxides to the 1.34 Å observed in this study.

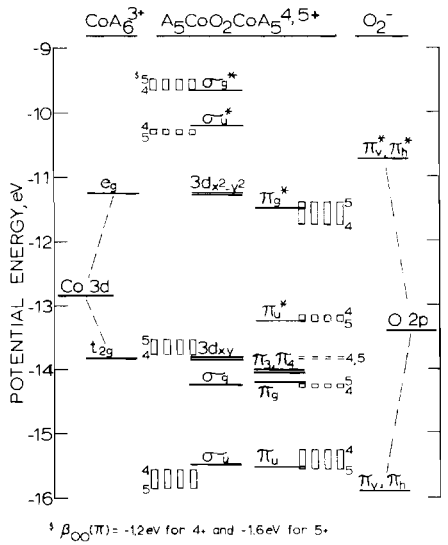

Fig. 7. Molecular orbital energy level diagram for CoO_2Co system. Assignments based on observed spectra are solid lines while dashed lines indicate Hückel calculated levels (*v.* Table VII).

Band *f* of the superoxo complex occurs at a slightly lower energy than bands *4* and *c* of the peroxo and mononuclear complexes, respectively. It may be identified as the $\sigma_u \rightarrow \sigma_g^*$ band also observed in the peroxo complex but shifted from 46,000 to 44,000 cm^{-1} due to the slight decrease in Co–O bonding energy as is suggested by the reduced *trans* effect. Miskowski *et al.* have attributed this band to $\pi_v \rightarrow \pi_v^*$ (analogous with our $\pi_u \rightarrow \pi_g^*$) but our assignment seems preferable in light of the ceiling for the energy of π_g^* being that of $3d_{x^2-y^2}$.

Table VI summarizes the observed bands and assignments.

Hückel Calculations

As a first attempt at a MO calculation upon a model for the CoO_2Co system consistent with the observed structures, it was assumed that simple Hückel calculations would show qualitative agreement between calculated eigenvalues and eigenvectors and the observed spectral properties, including EPR spectra [10, 17–21]. It was also assumed that such calculations could be performed for both the σ and π systems and that the results (summarized in Table VI) would be applicable to a single model for peroxo- and superoxo-bridged complexes.

In constructing the secular determinants, orbital interactions were assumed to occur as discussed above for the model and as shown in Figs. 5(a) and (b). The initial value for the cobalt coulomb integral was set at −12.8 eV, close to the −12.63 eV chosen by Hoffman *et al.* for the 3d orbitals of Fe^{2+} in extended Hückel calculations upon the modes of coordination in MX_2 and MO_2 [15]. This was subsequently split

TABLE VII. Summary of Hückel Calculations.

A. Sigma System

Orbital	Peroxide Eigenvalues (eV)	Superoxide Eigenvalues (eV)	Peroxide Eigenvectors Co($3d_{z^2}$)	Peroxide Eigenvectors O(2p)	Superoxide Eigenvectors Co($3d_{z^2}$)	Superoxide Eigenvectors O(2p)
σ_g^*	−9.64	−9.48	0.557	−0.435	0.536	−0.461
σ_u^*	−10.78	−10.34	0.642	−0.297	0.650	−0.279
σ_g	−13.76	−13.52	0.435	0.557	0.461	0.536
σ_u	−15.52	−15.86	0.297	0.642	0.279	0.650
			−11.2	−13.4	−11.2	−13.4
Coulomb Integrals (eV)		$\beta_{CoO}(\sigma)$	−2.0		−2.0	
Resonance Integrals		β_{OO}		−1.2		−1.6

B. Pi System

Orbital	Peroxide Eigenvalues	Superoxide Eigenvalues	Peroxide Eigenvectors Co($3d_{xz}$, $3d_{yz}$)	Peroxide Eigenvectors O(2p)	Superoxide Eigenvectors Co($3d_{xz}$, $3d_{yz}$)	Superoxide Eigenvectors O(2p)
π_g^*	−11.73	−11.40	−0.214	0.639	−0.189	0.655
π_u^*	−13.15	−13.26	−0.413	0.398	−0.435	0.349
π_4	−13.86	−13.86	0.069	0[a]	−0.638	0[a]
π_3	−13.86	−13.86	−0.704	0[a]	0.304	0[a]
π_g	−14.29	−14.22	0.452	0.303	0.463	0.267
π_u	−15.27	−15.56	0.281	0.584	0.247	0.615
			−13.86	−13.4	−13.86	−13.4
Coulomb Integrals (eV)		$\beta_{CoO}(\pi)$	−0.7, −0.7		−0.7, −0.7	
Resonance Integrals		β_{OO}		−1.2		−1.6

[a] In both π_3 and π_4, the eigenvector magnitudes are equivalent but not symmetric; π_3 is equivalent to π_4 by C_2 rotation as Co(1) interchanges with Co(1)′.

into 'e_g' and 't_{2g}' levels at −11.2 and −13.86 eV respectively, in agreement with the splitting in $Co(en)_3^{3+}$ [42]. The coulomb integral for oxygen initially was set at −13.6 eV, the first ionization potential for oxygen [43], and later was adjusted to −13.4 eV to obtain a better fit with spectroscopic assignments.

For both the σ and π systems, the resonance integral β_{OO} was set at −1.2 and at −1.6 eV, respectively, for the peroxo and superoxo complexes to account for variation in the dioxygen bond distance. The value of $\beta_{CoO}(\sigma)$ was varied until agreement was reached between the calculated and observed values for the $\sigma_u \rightarrow \sigma_g^*$ transition in the peroxo complex, yielding $\beta_{CoO}(\sigma) = -2.0$ eV. As shown in the orbital energy level diagram (Fig. 7), the observed energy level for σ_g differs markedly from that calculated. There are several explanations for these differences. First, possible participation of $3d_{xz}$ and $3d_{yz}$ in the sigma system had been ignored in favor of a single orbital on cobalt with which the dioxygen π_h and π_h^* would overlap. Second, rearrangement can be rationalized on the argument that dioxygen π_h^* orbitals should be significantly more effective in overlapping with the cobalt $3d_{z^2}$ than should π_h; this would stabilize σ_g at the expense of other orbitals within the planar system. Thirdly, there are the known limitations of the simple Hückel method. Nonetheless a value of $\beta_{CoO}(\sigma)$ which is consistent with other typical resonance integrals leads to a calculated energy difference between σ_u and σ_g^* which is close to those assigned from the spectra of the peroxide and superoxide complexes.

In considering possible values for $\beta_{CoO}(\pi)$, the energy of the vacant $3d_{x^2-y^2}$ orbital was set as an upper limit for the energy of π_g^*. Otherwise, $3d_{x^2-y^2}$ would become filled at the expense of π_g^*, contrary to structural and EPR information. With this limit on π_g^*, $\beta_{CoO}(\pi)$ cannot exceed approximately −0.7 eV and this value does yield eigenvalues in fair agreement with spectral assignments for the π system. As is often the case with simple Hückel calculations, the differences occurring between observed and calculated π energies are less than those for the σ system.

These Hückel parameters and results are listed in Table VII and the eigenvalues are as well included in Fig. 7.

Calculation of π spin density using the cobalt eigenvectors for π_g^* obtained with the Hückel parameters described above yields approximately 3.6% of the spin density on each cobalt. Duffy *et al.* have observed the electron ^{59}Co hyperfine coupling constant for $[(en)(dien)CoO_2Co(dien)(en)]^{5+}$ to be 11.0 gauss [17]. Using −90G as the hyperfine coupling constant for an electron in a 3d orbital of cobalt [10], the isotropic hyperfine coupling constant would be 1.2 G, well below the observed value. The coupling constant for an electron in a 4s orbital however is estimated to be 1320 G by Symons [44]. Thus hyperfine coupling would be much more sensitive to spin density in the sigma system than the pi.

In EPR studies of mononuclear cobalt–dioxygen adducts, Drago *et al.* conclude that spin polarization effects induced by the electron residing primarily in O_2 π_v^* are predominant and that the mechanism of coupling is mostly due to polarization of (dioxygen) electrons which are sigma donors to cobalt $3d_{z^2}$ [20]. They point out that it is the $3d_{z^2}$ rather than $3d_{xz}$ which can mix with the 4s to provide a means of extending spin density to the nucleus.

Our model seems to support the conclusions of Drago. Since both $3d_{xz}$ and $3d_{yz}$ place zero electron density at the nucleus, combinations of the two in the π system should be no more effective for hyperfine coupling than individual 3d orbitals. Furthermore, the 4s orbital cannot effectively combine with these 3d combinations to enhance π bonding while it can combine with $3d_{z^2}$ to enhance σ bonding. If hyperfine coupling does occur mainly to the extent of 4s involvement, then the polarization of the electrons in the σ system by the unpaired electron in the π system must be invoked. However, if $3d_{xz}$ and $3d_{yz}$ can participate in *both* the σ and π systems as was suggested earlier, then there is a means for inducing spin density in 4s which could be more effective than simple $\pi-\sigma$ polarization.

Acknowledgements

The authors wish to thank the following: Dr. David Duchamp of the Upjohn Company for collection of X-ray data, Kelvin Smith of Lawrence University for assistance in converting computer programs for use on the PDP-11/70, and Alma College for sabbatical leave support for R.C.B. The authors thank William P. Schaefer for kindly furnishing copies of Figs. 1 and 2 for our use.

Supplementary Material

Calculated and observed structure factors (10 pages). Ordering information is given on the masthead page of this journal.

References

1 University of Idaho, Moscow, Idaho, 83843.
2 J. R. Fritch, G. G. Christoph and W. P. Schaefer, *Inorg. Chem.*, *12*, 2170 (1973).
3 W. P. Schaefer and R. E. Marsh, *Acta Cryst.*, *21*, 735 (1966).
4 J. H. Timmons, A. Clearfield, A. E. Martell and R. H. Niswander, *Inorg. Chem.*, *17*, 1042 (1979).

5 J. H. Timmons, R. H. Niswander, A. Clearfield and A. E. Martell, *Inorg. Chem., 18,* 2977 (1979).
6 B. T. Huie, R. M. Leyden and W. P. Schaefer, *Inorg. Chem., 18,* 125 (1979).
7 N.-G. Vannerberg, *Acta Cryst., 18,* 449 (1965).
8 A. B. P. Lever, G. A. Ozin and H. B. Gray, *Inorg. Chem., 19,* 1823 (1980).
9 V. M. Miskowsi, J. L. Robbins, I. M. Treitel and H. B. Gray, *Inorg. Chem., 10,* 2318 (1975).
10 B. B. Wayland and M. E. Abd-Elmageed, *J. Am. Chem. Soc., 96,* 4809 (1974).
11 G. McLendon, S. R. Pickens and A. E. Martell, *Inorg. Chem., 16,* 1551 (1977).
12 M. Linhard and M. Weigel, *Z. Anorg. Chem., 308,* 254 (1961).
13 A. B. P. Lever and H. B. Gray, *Acc. Chem. Res., 11,* 348 (1978).
14 S. R. Pickens and A. E. Martell, *Inorg. Chem., 19,* 15 (1980).
15 R. Hoffman, M. M.-L. Chen and D. L. Thorn, *Inorg. Chem., 16,* 503 (1977).
16 J. Barrett, *Chem. Comm.,* 874 (1968).
17 D. L. Duffy, D. A. House and J. A. Weil, *J. Inorg. Nucl. Chem., 31,* 2053 (1969).
18 J. A. Weil and J. K. Kinnaird, *J. Phys. Chem., 71,* 3341 (1967).
19 B. M. Hoffman, D. L. Diemente and F. Basolo, *J. Am. Chem. Soc., 92,* 61 (1970).
20 B. S. Tovrog, D. J. Kitko and R. S. Drago, *J. Am. Chem. Soc., 98,* 5144 (1976).
21 M. Mori, J. A. Weil and J. D. Kinnaird, *J. Phys. Chem., 71,* 103 (1967).
22 I. Hyla-Krispin, L. Natkaniec and B. Jezowska-Trzebiatowska, *Bull. Acad. Pol. Sci. Ser. Sci. Chim., XXV,* 17 (1977).
23 R. C. Beaumont, *Dissertation Abstr., 29,* 1967-B (1968).
24 B. Bosnich, C. K. Poon and M. L. Tobe, *Inorg. Chem., 5,* 1514 (1966).
25 G. A. Lawrence and P. A. Lay, *J. Inorg. Nucl. Chem., 41,* 301 (1979).
26 C. Duval, 'Inorganic Thermogravimetric Analysis', Elsevier Publishing Co., New York, 1953, pp. 206–222.
27 H. J. Harwood, *J. Chem. Ed., 42,* 222 (1965).
28 R. G. Pearson, C. R. Boston and F. Basolo, *Phys. Chem., 59,* 304 (1955).
29 A. R. Gainsford and D. A. House, *Inorg. Chim. Acta, 3,* 367 (1969).
30 J. B. Work in 'Inorganic Syntheses', Vol. II, ed. by W. C. Fernelius, McGraw-Hill Book Co., Inc., New York, 1946, p. 221.
31 D. J. Duchamp, 'Algorithms for Chemical Computations', ACS Symposium Series, No. 46, 98 (1977).
32 'International Tables for X-ray Crystallography', Kynoch Press: Birmingham, England, 1962, Vol. III, p. 201.
33 C. K. Johnson, Report ORNL-3794, Oak Ridge National Laboratory, Oak Ridge, Tennessee, 1965.
34 R. Shiono, University of Pittsburgh.
35 R. B. Davidson, QCPE. Vol. X, Program No. 114, Indiana Univ., 1974.
36 J. P. Lowe, 'Quantum Chemistry'; Academic Press, Inc., New York, 1978, p. 246; (b) *ibid.,* pp. 181–190.
37 M. Ferrer, T. D. Hand and A. G. Sykes, *J. Chem. Soc. Dalton Trans.,* 14 (1980).
38 R. C. Elder and M. Trkula, *Inorg. Chem., 16,* 1048 (1977).
39 D. P. Bauer and R. S. Macomber, *Inorg. Chem., 15,* 1985 (1976).
40 G. B. Jameson, G. A. Rodley, W. T. Robinson, R. R. Gagne, C. A. Reed and J. P. Collman, *Inorg. Chem., 17,* 850 (1978).
41 V. Balzani and V. Carassiti, 'Photochemistry of Coordination Compounds', Academic Press, London, 1970.
42 C. K. Jørgensen, 'Absorption Spectra and Chemical Bonding in Complexes', Pergamon Press, London, 1962.
43 'Handbook of Chemistry and Physics'; 57th ed., CRC Press, Cleveland, 1976.
44 M. Symons, 'Chemical and Biochemical Aspects of Electron-Spin Resonance Spectroscopy'; John Wiley and Sons, New York, 1978.